

Elsevier instructions for the preparation of a 2-column format camera-ready paper in L^AT_EX

P. de Groot^{a*}, R. de Maas^{a†}, X.-Y. Wang^b and A. Sheffield^{a‡}

^aMathematics and Computer Science Section, Elsevier Science B.V.,
P.O. Box 103, 1000 AC Amsterdam, The Netherlands

^bEconomics Department, University of Winchester,
2 Finch Road, Winchester, Hampshire P3L T19, United Kingdom

These pages provide you with an example of the layout and style for 100% reproduction which we wish you to adopt during the preparation of your paper. This is the output from the L^AT_EX document class you requested.

1. FORMAT

Text should be produced within the dimensions shown on these pages: each column 7.5 cm wide with 1 cm middle margin, total width of 16 cm and a maximum length of 19.5 cm on first pages and 21 cm on second and following pages. The L^AT_EX document class uses the maximum stipulated length apart from the following two exceptions (i) L^AT_EX does not begin a new section directly at the bottom of a page, but transfers the heading to the top of the next page; (ii) L^AT_EX never (well, hardly ever) exceeds the length of the text area in order to complete a section of text or a paragraph. Here are some references: [1,2].

1.1. Spacing

We normally recommend the use of 1.0 (single) line spacing. However, when typing complicated mathematical text L^AT_EX automatically increases the space between text lines in order to prevent sub- and superscript fonts overlapping

*Footnotes should appear on the first page only to indicate your present address (if different from your normal address), research grant, sponsoring agency, etc. These are obtained with the `\thanks` command.

†For following authors with the same address use the `\addressmark` command.

‡To reuse an addressmark later on, label the address with an optional argument to the `\address` command, e.g. `\address[MCS]`, and repeat the label as the optional argument to the `\addressmark` command, e.g. `\addressmark[MCS]`.

one another and making your printed matter illegible.

1.2. Fonts

These instructions have been produced using a 10 point Computer Modern Roman. Other recommended fonts are 10 point Times Roman, New Century Schoolbook, Bookman Light and Palatino.

2. PRINTOUT

The most suitable printer is a laser or an inkjet printer. A dot matrix printer should only be used if it possesses an 18 or 24 pin printhead (“letter-quality”).

The printout submitted should be an original; a photocopy is not acceptable. Please make use of good quality plain white A4 (or US Letter) paper size. *The dimensions shown here should be strictly adhered to: do not make changes to these dimensions, which are determined by the document class.* The document class leaves at least 3 cm at the top of the page before the head, which contains the page number.

Printers sometimes produce text which contains light and dark streaks, or has considerable lighting variation either between left-hand and right-hand margins or between text heads and bottoms. To achieve optimal reproduction quality, the contrast of text lettering must be uniform,

sharp and dark over the whole page and throughout the article.

If corrections are made to the text, print completely new replacement pages. The contrast on these pages should be consistent with the rest of the paper as should text dimensions and font sizes.

3. TABLES AND ILLUSTRATIONS

Tables should be made with \LaTeX ; illustrations should be originals or sharp prints. They should be arranged throughout the text and preferably be included *on the same page as they are first discussed*. They should have a self-contained caption and be positioned in flush-left alignment with the text margin within the column. If they do not fit into one column they may be placed across both columns (using $\text{\begin{table*}}$ or $\text{\begin{figure*}}$ so that they appear at the top of a page).

3.1. Tables

Tables should be presented in the form shown in Table 1. Their layout should be consistent throughout.

Horizontal lines should be placed above and below table headings, above the subheadings and at the end of the table above any notes. Vertical lines should be avoided.

If a table is too long to fit onto one page, the table number and headings should be repeated above the continuation of the table. For this you have to reset the table counter with $\text{\addtocounter{table}{-1}}$. Alternatively, the table can be turned by 90° ('landscape mode') and spread over two consecutive pages (first an even-numbered, then an odd-numbered one) created by means of $\text{\begin{table}[h]}$ without a caption. To do this, you prepare the table as a separate \LaTeX document and attach the tables to the empty pages with a few spots of suitable glue.

3.2. Useful table packages

Modern \LaTeX comes with several packages for tables that provide additional functionality. Below we mention a few. See the documentation of the individual packages for more details. The

Table 2: The next-to-leading order (NLO) results *without* the pion field.

Λ (MeV)	140	150	175	200	225	250	Exp.	v_{18} [?]
r_d (fm)	1.973	1.972	1.974	1.978	1.983	1.987	1.966(7)	1.967
Q_d (fm ²)	0.259	0.268	0.287	0.302	0.312	0.319	0.286	0.270
P_D (%)	2.32	2.83	4.34	6.14	8.09	9.90	—	5.76
μ_d	0.867	0.864	0.855	0.845	0.834	0.823	0.8574	0.847
\mathcal{M}_{M1} (fm)	3.995	3.989	3.973	3.955	3.936	3.918	—	3.979
\mathcal{M}_{GT} (fm)	4.887	4.881	4.864	4.846	4.827	4.810	—	4.859
δ_{1B}^{VP} (%)	-0.45	-0.45	-0.45	-0.45	-0.45	-0.44	—	-0.45
$\delta_{1B}^{C2:C}$ (%)	0.03	0.03	0.03	0.03	0.03	0.03	—	0.03
$\delta_{1B}^{C2:N}$ (%)	-0.19	-0.19	-0.18	-0.15	-0.12	-0.10	—	-0.21

The experimental values are given in ref. [4].

Table 1
The next-to-leading order (NLO) results *without* the pion field.

Λ (MeV)	140	150	175	200
r_d (fm)	1.973	1.972	1.974	1.978
Q_d (fm ²)	0.259	0.268	0.287	0.302
P_D (%)	2.32	2.83	4.34	6.14
μ_d	0.867	0.864	0.855	0.845
\mathcal{M}_{M1} (fm)	3.995	3.989	3.973	3.955
\mathcal{M}_{GT} (fm)	4.887	4.881	4.864	4.846
δ_{1B}^{VP} (%)	-0.45	-0.45	-0.45	-0.45
$\delta_{1B}^{C2:C}$ (%)	0.03	0.03	0.03	0.03
$\delta_{1B}^{C2:N}$ (%)	-0.19	-0.19	-0.18	-0.15

The experimental values are given in ref. [4].

packages can be found in L^AT_EX's `tools` directory.

array Various extensions to L^AT_EX's `array` and `tabular` environments.

longtable Automatically break tables over several pages. Put the table in the `longtable` environment instead of the `table` environment.

dcolumn Define your own type of column. Among others, this is one way to obtain alignment on the decimal point.

tabularx Smart column width calculation within a specified table width.

rotating Print a page with a wide table or figure in landscape orientation using the `sidewaystable` or `sidewaysfigure` environments, and many other rotating tricks. Use the package with the `figuresright` option to make all tables and figures rotate in clockwise. Use the starred form of the `sideways` environments to obtain full-width tables or figures in a two-column article.

3.3. Line drawings

Line drawings may consist of laser-printed graphics or professionally drawn figures attached to the manuscript page. All figures should be clearly displayed by leaving at least one line of spacing above and below them. When placing a

figure at the top of a page, the top of the figure should align with the bottom of the first text line of the other column.

Do not use too light or too dark shading in your figures; too dark a shading may become too dense while a very light shading made of tiny points may fade away during reproduction.

All notations and lettering should be no less than 2 mm high. The use of heavy black, bold lettering should be avoided as this will look unpleasantly dark when printed.

3.4. PostScript figures

Instead of providing separate drawings or prints of the figures you may also use PostScript files which are included into your L^AT_EX file and printed together with the text. Use one of the packages from L^AT_EX's `graphics` directory: `graphics`, `graphicx` or `epsfig`, with the `\usepackage` command, and then use the appropriate commands (`\includegraphics` or `\epsfig`) to include your PostScript file.

The simplest command is:

`\includegraphics{file}`, which inserts the PostScript file `file` at its own size. The starred version of this command:

`\includegraphics*{file}`, does the same, but clips the figure to its bounding box.

With the `graphicx` package one may specify a series of options as a key-value list, e.g.:

```
\includegraphics[width=15pc]{file}
\includegraphics[height=5pc]{file}
\includegraphics[scale=0.6]{file}
\includegraphics[angle=90,width=20pc]{file}
```

See the file `grfguide`, section “Including Graphics Files”, of the `graphics` distribution for all options and a detailed description.

The `epsfig` package mimicks the commands familiar from the package with the same name in L^AT_EX2.09. A PostScript file `file` is included with the command `\psfig{file=file}`.

Grey-scale and colour photographs cannot be included in this way, since reproduction from the printed CRC article would give insufficient typographical quality. See the following subsections.



Figure 1. Good sharp prints should be used and not (distorted) photocopies.

3.5. Black and white photographs

Photographs must always be sharp originals (*not screened versions*) and rich in contrast. They will undergo the same reduction as the text and should be pasted on your page in the same way as line drawings.

3.6. Colour photographs

Sharp originals (*not transparencies or slides*) should be submitted close to the size expected in publication. Charges for the processing and printing of colour will be passed on to the

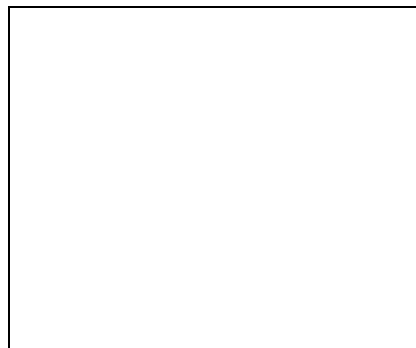


Figure 2. Remember to keep details clear and large enough.

author(s) of the paper. As costs involved are per page, care should be taken in the selection of size and shape so that two or more illustrations may be fitted together on one page. Please contact the Author Support Department at Elsevier (E-mail: authorsupport@elsevier.nl) for a price quotation and layout instructions before producing your paper in its final form.

4. EQUATIONS

Equations should be flush-left with the text margin; L^AT_EX ensures that the equation is preceded and followed by one line of white space. L^AT_EX provides the document class option `fleqn` to get the flush-left effect.

$$H_{\alpha\beta}(\omega) = E_{\alpha}^{(0)}(\omega)\delta_{\alpha\beta} + \langle \alpha | W_{\pi} | \beta \rangle \quad (1)$$

You need not put in equation numbers, since this is taken care of automatically. The equation numbers are always consecutive and are printed in parentheses flush with the right-hand margin of the text and level with the last line of the equation. For multi-line equations, use the `eqnarray` environment.

For complex mathematics, use the `AMSMath` package. This package sets the math indentation to a positive value. To keep the equations flush left, either load the `espcrc` package *after* the `AMSMath` package or set the command

`\mathindent=0pt` in the preamble of your article.

REFERENCES

1. S. Scholes, Discuss. Faraday Soc. No. 50 (1970) 222.
2. O.V. Mazurin and E.A. Porai-Koshits (eds.), Phase Separation in Glass, North-Holland, Amsterdam, 1984.
3. Y. Dimitriev and E. Kashchieva, J. Mater. Sci. 10 (1975) 1419.
4. D.L. Eaton, Porous Glass Support Material, US Patent No. 3 904 422 (1975).

References should be collected at the end of your paper. Do not begin them on a new page unless this is absolutely necessary. They should be prepared according to the sequential numeric system making sure that all material mentioned is generally available to the reader. Use `\cite` to refer to the entries in the bibliography so that your accumulated list corresponds to the citations made in the text body.

Above we have listed some references according to the sequential numeric system [1–4].

Stability of two-fermion bound states in the explicitly covariant Light-Front Dynamics

M. Mangin-Brinet,^aJ. Carbonell^a and V. A. Karmanov^b

^aInstitut des Sciences Nucléaires,
53, avenue des Martyrs, 38 026 Grenoble, France

^bLebedev Physical Institute,
Leninsky Pr. 53, 119991 Moscow, Russia

1. Introduction

The system of two bound fermions covers a huge number of interesting problems from atomic, nuclear and subnuclear physics. It is one of the most difficult problems in field theory due to the fact that bound states necessarily involve an infinite number of diagrams. We studied this problem in the framework of the explicitly covariant light-front dynamics [1] (CLFD). In this approach, the state vector is defined on an hyperplane given by the invariant equation $\omega \cdot x = 0$ with $\omega^2 = 0$. The standard light-front, reviewed in [2], is recovered for $\omega = (1, 0, 0, -1)$. The CLFD equations have been solved exactly for a two fermion system with different boson exchange ladder kernels [3,4]. We have considered separately the usual couplings between two fermions (scalar, pseudo-scalar, pseudo-vector, and vector) and we were interested in states with given angular momentum and parity $J^\pi = 0^\pm, 1^\pm$. Each coupling leads to a system of integral equations, which in practice are solved on a finite momentum domain $[0; k_{max}]$. If the solutions necessarily exist when the integration domain is finite – for the kernels are compact, it is not a priori obvious that the equations admit stable solutions when k_{max} goes to infinity. Particular attention must therefore be paid to the stability of the equations relative to the cutoff k_{max} . We develop hereafter an analytical method to study the cutoff dependence of the equations and to determine whether they need to be regularized or not.

The method will here be detailed for a $J = 0^+$ state in the Yukawa model but it can be applied to any coupling. Results will be presented for scalar and pseudo-scalar exchange. This latter furthermore exhibits some strange particularities which will be discussed.

2. Scalar exchange

Let us consider a system of two fermions in a $J^\pi = 0^+$ state, bound by a scalar exchange, whose Lagrangian density is given by $\mathcal{L} = g_s \bar{\Psi} \Phi \Psi$. Its wave function, constructed using all possible spin structures, is determined in the 0^+ case by two components [6], f_1 and f_2 , which depend on the two scalar variables k and θ :

$$\psi = \frac{1}{\sqrt{2}} w_{\sigma_2}^\dagger \left(f_1 + i \frac{\vec{\sigma} \cdot [\vec{k} \times \hat{n}]}{k \sin \theta} f_2 \right) \sigma_y w_{\sigma_1}^\dagger$$

\vec{k} is the momentum of one particle in the system of reference where $\vec{k}_1 + \vec{k}_2 = 0$, \hat{n} is the spatial part of the normal ω to the light-front plane, θ is the angle between \vec{k} and \hat{n} , and w is the two component spinor. The appearance of a second component compared to the non relativistic case is due to vector \hat{n} , which induces additional spin structures.

f_1 and f_2 satisfy the system of coupled equations :

$$\begin{aligned} & [M^2 - 4(k^2 + m^2)] f_1(k, \theta) \\ &= \frac{m^2}{2\pi^3} \int [K_{11} f_1(k', \theta') + K_{12} f_2(k', \theta')] \frac{d^3 k'}{\varepsilon_{k'}} \end{aligned}$$

$$\begin{aligned} & [M^2 - 4(k^2 + m^2)] f_2(k, \theta) \\ &= \frac{m^2}{2\pi^3} \int [K_{21} f_1(k', \theta') + K_{22} f_2(k', \theta')] \frac{d^3 k'}{\varepsilon_{k'}} \quad (1) \end{aligned}$$

M^2 is the total mass squared of the system, m is the constituent mass and $\varepsilon_k = \sqrt{k^2 + m^2}$. The kernels K_{ij} result from a first integration of more elementary quantities:

$$K_{ij}(k, \theta; k', \theta') = \int_0^{2\pi} \frac{\kappa_{ij}}{(Q^2 + \mu^2)m^2 \varepsilon_k \varepsilon_{k'}} \frac{d\varphi'}{2\pi},$$

where κ_{ij} depend on the type of coupling. The analytical expressions of κ_{ij} for the scalar coupling, read

$$\begin{aligned} \kappa_{11}^S &= -\alpha\pi [2k^2 k'^2 + 3k^2 m^2 + 3k'^2 m^2 + 4m^4 \\ &\quad - 2kk' \varepsilon_k \varepsilon_{k'} \cos \theta \cos \theta' \\ &\quad - kk'(k^2 + k'^2 + 2m^2) \sin \theta \sin \theta' \cos \varphi'] \\ \kappa_{12}^S &= -\alpha\pi m(k^2 - k'^2) (k' \sin \theta' + k \sin \theta \cos \varphi') \\ \kappa_{21}^S &= -\alpha\pi m(k'^2 - k^2) (k \sin \theta + k' \sin \theta' \cos \varphi') \\ \kappa_{22}^S &= -\alpha\pi [(2k^2 k'^2 + 3k^2 m^2 + 3k'^2 m^2 + 4m^4 \\ &\quad - 2kk' \varepsilon_k \varepsilon_{k'} \cos \theta \cos \theta') \cos \varphi' \\ &\quad - kk'(k^2 + k'^2 + 2m^2) \sin \theta \sin \theta'] \quad (2) \end{aligned}$$

In practice, the integration region over the momenta is reduced to a finite domain $[0, k_{max}]$. The kinematical term $[M^2 - 4(k^2 + m^2)]$ on l.h.s. of equation (1) does not generate any singularity and the kernels K_{ij} are smooth functions of the θ variable. Thus, the stability of the solution depends only on the asymptotical behavior of the kernels in the (k, k') plane.

Variables (k, k') can tend to infinity following different directions: for a fixed value of k , K_{11} decreases as $1/k'$, and vice versa. As the integration volume contains the factor $\varepsilon_{k'}$, this means that the total kernel decreases as $1/k'^2$, that is like a Yukawa potential. In contrast, K_{22} does not decrease in any direction of the (k, k') plane, but tends to a positive constant with respect to k and k' . K_{22} is thus asymptotically repulsive and does not generate any unstability. In the domain where both k, k' tend to infinity with a fixed ratio $\frac{k'}{k} = \gamma$, it is useful to introduce the functions A_{ij} defined by

$$K_{ij} = -\frac{\pi\alpha}{m^2} \begin{cases} \sqrt{\gamma} A_{ij}(\theta, \theta', \gamma) & \text{if } \gamma \leq 1 \\ \frac{1}{\sqrt{\gamma}} A_{ij}(\theta, \theta', 1/\gamma) & \text{if } \gamma \geq 1 \end{cases}$$

Since K_{22} is repulsive and does not generate any collapse, we consider only the first channel. We have

$$\begin{aligned} A_{11}(\theta, \theta', \gamma) &= \frac{1}{\sqrt{\gamma}} \int_0^{2\pi} \frac{d\varphi'}{2\pi} \frac{1}{D} \times \\ &\{2\gamma(1 - \cos \theta \cos \theta') - (1 + \gamma^2) \sin \theta \sin \theta' \cos \varphi'\} \end{aligned}$$

where

$$\begin{aligned} D &= (1 + \gamma^2)(1 + |\cos \theta - \cos \theta'| - \cos \theta \cos \theta') \\ &\quad - 2\gamma \sin \theta \sin \theta' \cos \varphi' \end{aligned}$$

Let us now majorate the function A_{11} . For fixed γ , the maximum of A_{11} is achieved at $\theta = \theta'$ and for any $\theta = \theta'$ it reads: $A_{11}(\theta = \theta', \gamma) = \alpha' \sqrt{\gamma}$. The maximum value of kernel K_{11} is thus reached for $\gamma = 1$. The majorated kernel obtained this way coincides with the non-relativistic potential $U(r) = -\alpha'/r^2$ in the momentum space with $\alpha' = \alpha/(2m\pi)$. As well known [7], for this potential, the binding energy does not depend on cutoff if $\alpha' < \alpha_{cr} = 1/(4m)$ what restricts the coupling constant to: $\alpha < \pi/2$. If $\alpha' > 1/(4m)$, the binding energy is cutoff dependent and tends to $-\infty$ when $k_{max} \rightarrow \infty$. A finer majoration of A_{11} was done by taking into account its dependence on γ [8]. In this way we have found $\alpha_{cr} = \pi$, instead of $\pi/2$. As the kernel was majorated, the critical coupling constant is expected to be larger than π .

It can be determined, together with the asymptotical behavior of the wave functions, by considering the limit $k \rightarrow \infty$ of equation (1) for f_1

$$\begin{aligned} -4f(k, z) &= \\ &\frac{m^2}{\pi^2} \int_0^\infty \gamma d\gamma \int_{-1}^{+1} dz' K(k, z; \gamma k, z') f(\gamma k, z') \end{aligned}$$

where we have neglected the binding energy, supposing that it is finite, and omitted the indices for f_1 and K_{11} . This can also be written

$$\begin{aligned} 4f(k, z) &= \frac{\alpha}{\pi} \int_{-1}^1 dz' \int_0^1 d\gamma A(\theta, \theta', \gamma) \\ &\times \left\{ \gamma^{3/2} f(\gamma k, z') + \gamma^{-5/2} f\left(\frac{k}{\gamma}, z'\right) \right\} \quad (3) \end{aligned}$$

Looking for a solution which behaves as

$$f(k, z) \sim \frac{h(z)}{k^{2+\beta}}, \quad 0 \leq \beta < 1. \quad (4)$$

we are led for $h(z)$ to the eigenvalue equation

$$h(z) = \alpha \int_{-1}^{+1} dz' H_\beta(z, z') h(z')$$

with

$$H_\beta(z, z') = \int_0^1 \frac{d\gamma}{2\pi\sqrt{\gamma}} A(z, z', \gamma) \cosh(\beta \log \gamma)$$

The relation between the coupling constant α and the coefficient β , determining the power law of the asymptotic wave function, can be found in practice by solving the eigenvalue equation (5) for a fixed value of β

$$\lambda_\beta h(z) = \int_{-1}^{+1} dz' H_\beta(z, z') h(z') \quad (5)$$

and taking $\alpha(\beta) = 1/\lambda_\beta$. The relation $\alpha(\beta)$ obtained that way is represented in Figure 1. The value $\beta = 0$ corresponds to the maximal – that is the critical – value of α : $\alpha_c = \alpha(\beta = 0) = 3.72$, in agreement with the previous analytical estimations. It is independent of the exchanged mass μ .

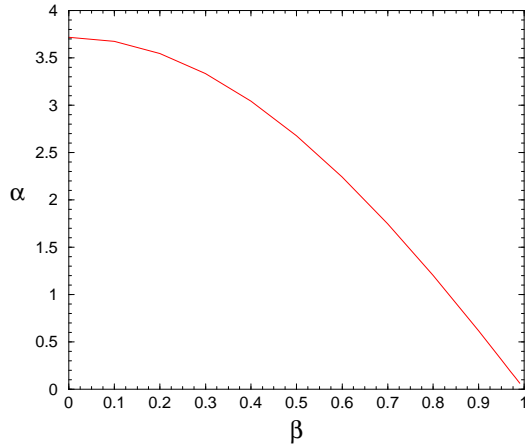


Figure 1. Function $\alpha(\beta)$ for LFD Yukawa model with K_{11} channel only.

Figure 2 shows the two different regimes, whether the coupling constant is below ($\alpha = 3$) or above ($\alpha = 4$) the critical value α_c . As it can be seen in Figure 3, the wave functions accurately follow the power law asymptotical behavior

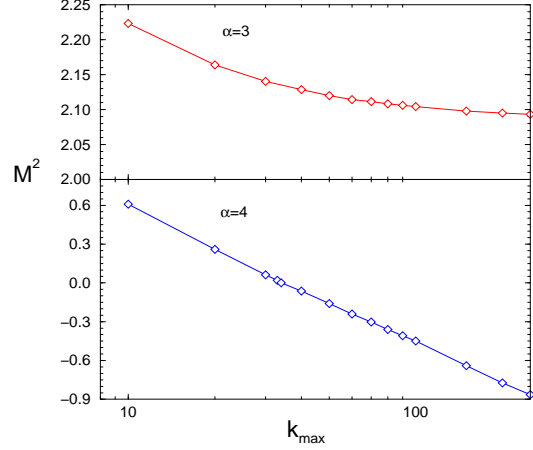


Figure 2. Cutoff dependence of the binding energy in the $J = 0^+$ state ($\mu = 0.25$), in the one-channel problem (f_1), for two fixed values of the coupling constant below and above the critical value.

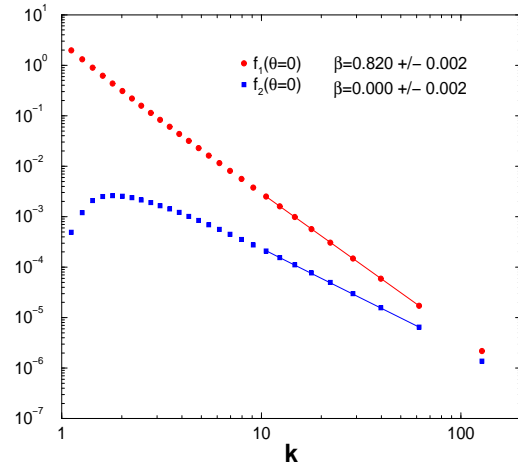


Figure 3. Asymptotical behavior of the $J = 0^+$ wave function components f_i for $B=0.05$, $\alpha=1.096$, $\mu=0.25$. The slope coefficient are $\beta_1 = 0.82$ and $\beta_2 \approx 0$.

$1/k^{2+\beta}$ with a coefficient $\beta(\alpha)$ given in Figure 1. It is worth noticing that – at least in the framework of this model – one could measure the coupling constant from the asymptotic behavior of the bound state wave function.

A similar study has been done for the $J = 1^+$ state, which is shown to be unstable without regularization [8,9].

3. Pseudo-scalar coupling

The stability of the pseudo-scalar (PS) coupling is analyzed similarly to the scalar one. The same method leads to the conclusion that the equations for the PS coupling are quite surprisingly stable without any regularization.

However, the results show a "quasi-degeneracy" of the coupling constant, for a wide range of binding energies. One has for instance (see Figure 4) $\alpha = 49.5$ for a system with $B = 0.001$, and $\alpha = 48.6$ for a system five hundred times more deeply bound ($B = 0.5$), that is only a 2% difference.

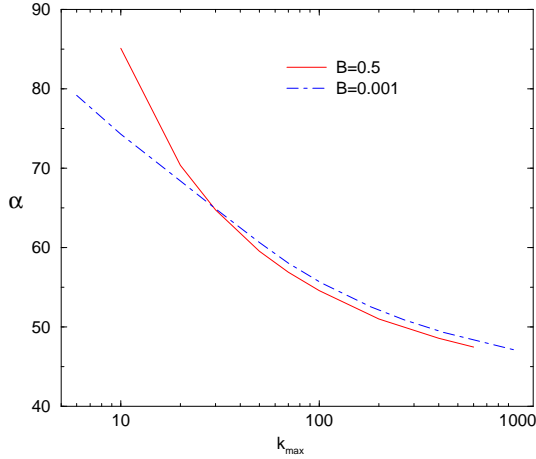


Figure 4. Convergence of coupling constants as function of the cutoff k_{max} for $B = 0.001$ and $B = 0.5$. The exchange mass is $\mu = 0.15$.

This peculiar behavior can be shown to come from the second channel:

$$[M^2 - 4(k^2 + m^2)]f_2(k, \theta) =$$

$$\frac{m^2}{2\pi^3} \int K_{22}^{PS}(k, k', \theta, \theta', M^2) f_2(k', \theta') \frac{d^3 k'}{\varepsilon_{k'}} \quad (6)$$

The kernel $K_{22}(k, k', \theta, \theta', M^2)$, whose expression is explicitly given in [3], is represented in Figure 5 for fixed values of θ, θ' . It vanishes for $k = 0$ or $k' = 0$ and tends towards a positive constant in all the (k, k') plane.

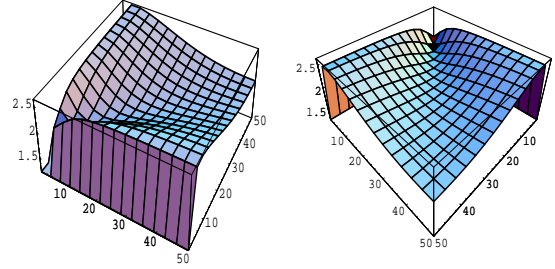


Figure 5. K_{22} kernel in (k, k') plane.

Let us modelize this kernel by a kind of "potential barrier" in the momentum space (k, k') , displayed in Figure 6, whose advantage is to be analytically solvable.

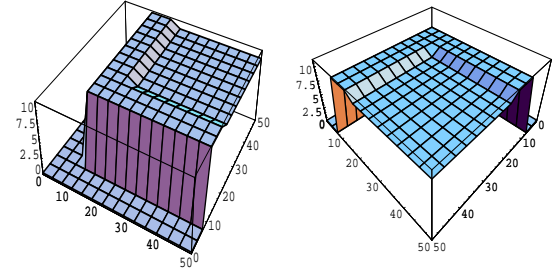


Figure 6. Modelization of K_{22} by a simpler kernel in the (k, k') plane.

$$\begin{aligned} K(k, k') &= \frac{\alpha U_1}{m^2} \Theta(k' - k_1) \Theta(k_2 - k') \\ &\times [\Theta(k - k_1) \Theta(k_2 - k) + \Theta(k - k_2) \Theta(k_{max} - k)] \\ &+ \Theta(k' - k_2) \Theta(k_{max} - k') \left[\frac{\alpha U_1}{m^2} \Theta(k - k_1) \right. \\ &\left. \times \Theta(k_2 - k) + \frac{\alpha U_2}{m^2} \Theta(k - k_2) \Theta(k_{max} - k) \right] \end{aligned}$$

with $\Theta(x) = 1, x > 0$ and $\Theta(x) = 0, x \leq 0$. This kernel has the same characteristics than K_{22}^{PS}

since it is zero when $k, k' \rightarrow 0$, and tends towards a constant when (k, k') go to infinity with a fixed ratio $\gamma = k'/k$.

f_2 satisfies the Schrödinger type equation

$$[k^2 + \kappa^2]f_2(k) = -\frac{m^2}{(2\pi)^3} \int K(k, k')f_2(k') \frac{d^3k'}{k'} \quad (7)$$

with $\kappa^2 = m^2 - \frac{M^2}{4}$. We assume that $k_1 < k_2 < k_{max}$ et $U_2 < U_1$. The term $\varepsilon_{k'}$ in the volume element of (6) was replaced by its large momentum behavior, that is by k' . We define $\Gamma(k) = [k^2 + \kappa^2]f_2(k)$. The equation for $\Gamma(k)$, which is analytically solvable, reads:

$$\Gamma(k) = -\frac{m^2}{2\pi^2} \int_{-\infty}^{+\infty} K(k, k') \frac{\Gamma(k')}{k'^2 + \kappa^2} k' dk'$$

The solution $\Gamma(k)$ is constant for $k_1 < k < k_2$ and $k_2 < k < k_{max}$:

$$\begin{aligned} \Gamma(k) &= \Gamma_1 \Theta(k - k_1) \Theta(k_2 - k) \\ &+ \Gamma_2 \Theta(k - k_2) \Theta(k_{max} - k) \end{aligned}$$

The Γ_i satisfy the coupled equations

$$\begin{cases} (1 + \alpha u_1 a) \Gamma_1 &= -\alpha u_1 b \Gamma_2 \\ (1 + \alpha u_2 b) \Gamma_2 &= -\alpha u_1 a \Gamma_1 \end{cases}$$

where we have defined $u_i = \frac{m^2}{2\pi^2} U_i$ and

$$a = \log \left(\frac{k_2^2 + \kappa^2}{k_1^2 + \kappa^2} \right), \quad b = \log \left(\frac{k_{max}^2 + \kappa^2}{k_2^2 + \kappa^2} \right) \quad (8)$$

Replacing $\Gamma(k)$ by its definition in terms of $f_2(k)$, we finally get the solution of equation (7) on the form:

$$\begin{aligned} f_2(k) &= \frac{N}{k^2 + \kappa^2} [\Theta(k - k_1) \Theta(k_2 - k) \\ &- \frac{\alpha a u_1}{(1 + \alpha b u_2)} \Theta(k - k_2) \Theta(k_{max} - k)] \end{aligned}$$

where N is a normalisation constant. For a given κ the coupling constant is

$$\alpha(\kappa) = \frac{(a u_1 + b u_2) + \sqrt{(a u_1 - b u_2)^2 + 4 u_1^2 a b}}{2 a b u_1 (u_1 - u_2)}$$

and the results provided by this simple kernel are summarized in Table 1. $\alpha(\kappa)$ depends on κ through logarithms in a, b , eq. (8). Besides, the

Table 1

Coupling constant as a function of the binding energy for the analytical model of the PS coupling second channel.

B	α
0.001	22.5327
0.010	22.5334
0.100	22.5396
0.500	22.5639
1, 00	22.5862
1.50	22.5995
2.00	22.6040

value of κ is much smaller than k_1, k_2, k_{max} . This explains the very weak dependence of $\alpha(\kappa)$ v.s. κ .

We conclude from the above discussion that, even if the PS coupling does not formally need any regularization to insure its stability, calculations without form factors – though analytically understood – lead to results which are hardly interpretable on the physical point of view.

Acknowledgements: The numerical calculations were performed at CGCV (CEA Grenoble) and IDRIS (CNRS). We are grateful to the staff members of these two organizations for their constant support.

REFERENCES

1. V.A. Karmanov, ZhETF 71 (1976) 399 (transl.: JETP 44 (1976) 210).
2. S.J. Brodsky, H.-C. Pauli and S.S. Pinsky, Phys. Rep., **301** (1998) 299.
3. M. Mangin-Brinet, *Thèse Université de Paris* (2001).
4. M. Mangin-Brinet, J. Carbonell and V.A. Karmanov, submitted for publication.
5. J. Carbonell, B. Desplanques, V.A. Karmanov and J.-F. Mathiot, Phys. Reports 300 (1998) 215.
6. J. Carbonell and V.A. Karmanov, Nucl. Phys. A589 (1995) 713.
7. L.D. Landau, E.M. Lifshits, *Quantum mechanics*, §35, Pergamon press, 1965.
8. M. Mangin-Brinet, J. Carbonell and V.A. Karmanov, Phys Rev D 64 (2001) 027701.
9. M. Mangin-Brinet, J. Carbonell and V.A. Karmanov, accepted in Phys Rev D (2001).